Determination of ethyl octanoate in Chinese liquor using FT-NIR spectroscopy

[1,2]*Liu, J., [1]Dong, X., [1,2]Han, S., [1,2]Xie, A., [1,2]Li, X., [1,2]Li, P., [1,2]Xu, B. and [1,2]Luo, D.

[1]College of Food and Bioengineering, Henan University of Science and Technology, Luoyang, China
[2]Henan Engineering Research Centre of Food Material, Luoyang, China

Abstract

To quantitatively detect ethyl octanoate in Chinese liquor, Fourier-transform near-infrared (FT-NIR) spectroscopy was performed in the present work, with 162 Chinese liquor samples selected from Luoyang Dukang Distillery. The chemical values of ethyl octanoate were determined by gas chromatography (GC), and spectral data from 12,000 to 4000 cm^{-1} were collected. The calibration model was established with partial least squares (PLS) regression, and then validated using internal cross-validation. The predictability of the model was further confirmed by the validation set as external validation. After comparing the effects of the models set up with sample data under different pre-processing methods, the model was built within the spectral region of 6101.7 - 5449.8 cm^{-1}; based on the SNV pre-processing method which was selected as the optimal model. The coefficient of determination (R^2) for cross-validation of the model was 0.9507, and the corresponding root mean square errors of cross-validation (RMSECV) was 3.91 mg L^{-1}. The R^2 for external validation was 0.9537, and the root mean square errors of prediction (RMSEP) was 3.62 mg L^{-1}. The results demonstrated that using NIR spectroscopy to determine ethyl octanoate in Chinese liquor is feasible and can achieve satisfactory results.

Introduction

Chinese liquor is a traditional spirit (Liu and Sun, 2018) distilled from sorghum, wheat, corn, rice, glutinous rice, and other grains; and goes through the processes of cooking, saccharifying, fermenting, distilling, storing, and blending. During liquor fermentation and distillation, a large number of flavour compounds including alcohols, acids, esters, phenols, ketones, acetals, nitrogenous compounds, and sulphur compounds are produced (Zheng *et al.,* 2016). Although these compounds account for a small portion of liquor, they play an essential role in liquor flavour and quality. To produce high-quality liquor with appealing flavour and strong aroma, it is necessary to determine the most appropriate concentration ratio among these flavour compounds. Therefore, investigating flavour-producing substances plays a critical role in flavour type innovation and process improvement of liquor. Ethyl caproate is generally considered the main component of strong-aroma type liquor, and it works with ethyl butyrate, ethyl acetate, and ethyl lactate to form the four major esters of strong-aroma type liquor. Moreover, in the blending process of strong-aroma type liquor, the ratio of the four esters requires special attention for better coordination. With continuous development of modern

technologies, more trace flavour compounds have been discovered in liquor, including ethyl octanoate. Ethyl octanoate plays a significant role in strong-aroma type liquor; its aroma intensity is much higher than that of ethyl acetate and ethyl lactate, and is second only to ethyl caproate. Therefore, it is important to achieve rapid determination of ethyl octanoate in Chinese liquor (Wang *et al.,* 2014).

A typical method for analysing flavour compounds in liquor is gas chromatography (GC) or its combination with other techniques, including stir bar sorption extraction (SBSE) coupled with gas chromatography-mass spectrometry (GC-MS) (Fan *et al.,* 2011), gas chromatography-olfactometry (GC-O) and GC-MS (Fan *et al.,* 2012; Gao *et al.,* 2014), solid-phase micro extraction (SPME) and GC-MS (Wang *et al.,* 2015), SBSE, thermal desorption system (TDS), and GC-MS (Niu *et al.,* 2015), GC-flame photometric detection (FPD) (Niu *et al.,* 2017), and headspace (HS)-SPME and GC-pulsed flame photometric detection (PFPD) (Sha *et al.,* 2016). Although these methods are accurate and sensitive, the implementation procedures are cumbersome and time-consuming, and they cannot be applied to rapid detection of liquor in the liquor industry. To meet actual production needs, a simple and fast online analysis technology is required. In such a case, near-infrared

spectroscopy (NIRS) is a suitable choice.

Near infrared spectroscopy is a rapid, convenient, non-destructive, and environmentally friendly technology, widely used for simultaneous detection of multiple components in the food industry (Adedipe *et al.,* 2016; Bernhard *et al.,* 2016; Zhong and Qin, 2016). NIRS has also greatly contributed to the alcoholic beverage industry, where it is applied for rapid determination of the parameters in the fermentation process of alcoholic beverages (Grassi *et al.,* 2014; Wu *et al.,* 2015a; 2015b), for classification and identification of liquor (Fei *et al.,* 2012; Chen *et al.,* 2014; Li *et al.,* 2014), and for analyses of conventional physical and chemical indicators of liquor (Lorenzo *et al.,* 2009; Martelovidal and Vázquez, 2014; Ye *et al.,* 2014; Ouyang *et al.,* 2015). However, there have been few reports on the determination of ethyl octanoate in Chinese liquor by NIRS.

In the present work, Dukang liquor, a strong-aroma type liquor, was selected to study the content of ethyl octanoate, which was determined by GC-flame ionisation detector (FID). Then, the near-infrared (NIR) spectrum of liquor was scanned and analysed, and the mathematical relationship between the chemical value and spectrum was established by the partial least squares (PLS) method. The feasibility of rapid determination of ethyl octanoate in liquor by NIRS was explored.

Materials and methods

Materials and chemicals

A total of 162 Chinese liquor samples were obtained from Luoyang Dukang Holdings Ltd. (Henan province, China) as the original distillate. The samples were collected from different fermentation pools, and at different distillation phases in the liquor production line. All liquor samples were stored at 4°C until analysis. Ethyl octanoate of the GC standard (purity ≥ 99%) was purchased from Aladdin Bio-Chem Technology Co., Ltd (Shanghai, China), and absolute ethanol was from Kermel Chemical Reagent Co., Ltd (Tianjin, China).

Ethyl octanoate (0.1 mL) was transferred into a 100 mL volumetric flask and diluted with 600 mL L^{-1} ethanol to obtain standard stock solution (1 mL L^{-1}). A volume of 10 mL of calibration standards with 600 mL L^{-1} ethanol was prepared by the dilution of 0.1, 0.25, 0.5, 1, 2, and 3 mL standard stock solution at six gradient concentrations, respectively.

Gas chromatography

The GC analysis was carried out using an Agilent 7890A gas chromatography system, equipped with a flame ionisation detector (Agilent Technologies, Inc., USA). Separation was performed with a silica capillary column AT.LZP-930 (25 m × 0.53 mm × 1 μm; Lanzhou Institute of Chemical Physics, Chinese Academy of Sciences). Nitrogen (99.999% purity) was employed as the carrier gas, and maintained at a flow rate of 30 mL min^{-1}, by being injected for a volume of 1 μL with a split ratio of 10:1. The injector and detector temperatures were set at 220 and 250°C, respectively. The chromatographic program was set at 75°C, held for 3 min, and then raised to 210°C at a step of 10°C min^{-1}. The total GC run time was 16.5 min.

NIR spectrum acquisition

All spectra from the liquor were acquired using a Fourier transform near-infrared (FT-NIR) spectrometer VECTOR33 (Bruker Corporation, Germany). Before measurements, the FT-NIR instrument was pre-heated for 30 min. After the instrument passed the test, air was used as the reference, and the quartz cuvette was selected with the optical path of 1 mm, and background scanning was carried out at first. Based on the characteristics of the liquor samples, the transmission mode was used to collect the spectra. The ambient temperature was equilibrated at 25 ± 2°C for spectrum acquisition. The spectral scanning range was 12,000 - 4000 cm^{-1}, the instrument resolution was 8 cm^{-1}, and each sample was obtained by an average of 32 scans. The sample spectra were analysed using OPUS 8.1 software (Bruker Optics Inc., Germany).

Spectrum processing

Raw spectra of the samples should be pre-processed to reduce external interference, minimise baseline variation, and increase spectral differences. In order to achieve the highest accuracy and reliability of the prediction model, different pre-processing methods were applied, including straight line subtraction (SLS), standard normal variate (SNV), min-max normalisation (MMN), multiplicative scatter correction (MSC), first derivative (D1), and second derivative (D2) (Egidio *et al.,* 2010). Besides, spectral region selection for optimal modelling has a profound impact on the quality of the multivariate calibration model. The NIR full-spectra data have a large volume and contain much interference information unrelated to the prediction target, and the characteristic spectral region needs to be filtered. The OPUS software has a set of five NIR frequency regions for the optimised models: 9400 - 7500, 7500 - 6100, 6100 - 5450, 5450

- 4600, and 4600 - 4250 cm^{-1}. By combining these pre-processing methods and spectral regions, the optimal band and best pre-processing method can be identified (Callado *et al.,* 2018).

Establishment of the models and evaluation standards

Partial least squares (PLS) regression was utilised to establish a mathematical model for predicting the content of ethyl octanoate. The PLS regression is based on simultaneous decomposition of the spectral matrix (X) and concentration matrix (Y), which gradually extracts the components (usually referred to as PLS factors) from the data, and verifies the significance of the model until it meets the requirements. The PLS regression algorithm can use part or all of the spectra as variables to establish a quantitative analysis model of NIRS. PLS regression is the most commonly used multivariate calibration method in quantitative analysis, which overcomes the collinearity, band overlap, data interference, and other common problems. All samples were randomly divided into a calibration set and validation set at a ratio of 3:1. The calibration model was established using samples in the calibration set, where internal cross-validation was performed, and then external verification was performed with samples in the validation set. The optimal model was determined based on indicators such as the coefficient of determination (R^2), root mean square errors of cross-validation (RMSECV), and root mean square errors of prediction (RMSEP). A good model should have lower RMSECV and RMSEP, and higher R^2, with a small disparity between RMSECV and RMSEP (Aleixandre-Tudo *et al.,* 2018). R^2, RMSECV, and RMSEP were calculated using Eq.1, Eq.2 and Eq.3, respectively:

$$R^2 = 1 - \frac{\sum_{i=1}^{n}(y_i - \hat{y}_i)^2}{\sum_{i=1}^{n}(y_i - \overline{y})^2} \qquad (Eq. 1)$$

where, n = number of samples; y_i = reference measurement value of sample i; y_i = predicted value of sample i; and y = mean of the reference measurement values.

$$RMSECV = \sqrt{\left(\sum_{i=1}^{n} \frac{(y_i - \hat{y}_i)^2}{n}\right)} \qquad (Eq. 2)$$

where, n = number of samples in the calibration set; y_i = reference measurement value of sample i; and y_i = predicted value of sample i.

$$RMSEP = \sqrt{\left(\sum_{i=1}^{n} \frac{(y_i - \hat{y}_i)^2}{n}\right)} \qquad (Eq. 3)$$

where, n = number of samples in the validation set; y_i = reference measurement value of sample i; and y_i = predicted value of sample i.

Results and discussion

Chemical analysis

The 162 liquor samples were analysed by GC-FID, and the analysis results of the distribution of the ethyl octanoate content in liquor are shown in Table 1. Since the liquor samples were from different fermentation pools, the ethyl octanoate content in the samples covered a relatively wide range. The range of the validation set was included in the larger range of the calibration set. In addition, different concentrations of ethyl octanoate were evenly distributed in the two data set, which was suitable for building a good NIR model.

NIR spectra of Chinese liquor

The original spectra of the liquor samples are shown in Figure 1(A). There were a total of 2025 variables (data points) with the wavenumbers ranging from 12,000 to 4000 cm^{-1}. The spectral curve could be explained by the overtones of different functional groups in the samples. The spectral changes of all the samples were basically the same, and no abnormal values could be found with naked eyes. Although PLS could tolerate full-band modelling, the models' short-wavelength regions were relatively flat with no sufficient spectral information. If an excessively wide band range is selected, it contains much redundant information. This will damage the performance of the model, as it will increase the calculation time, and even reduce the prediction effect of the model. Therefore, avoiding short-wavelength regions is recommended for spectral region selection. The spectra had two large absorption bands at 6896 and 5128 cm^{-1}, which were ascribed to the O-H first overtone and O-H

Table 1. Ethyl octanoate content in calibration and validation sets (mg L^{-1}).

Subset	Number of sample	Range	Mean	SD
Calibration set	121	15.50 - 89.00	56.13	17.68
Validation set	41	24.16 - 88.83	54.29	17.05

SD: standard deviation.

combination band in water molecules, respectively. There was also a small absorption band at 10,416 cm^{-1}, which was related to the O-H second overtone (Chu *et al.*, 2014; Wu *et al.*, 2015c). In order to obtain a model with high stability and accuracy, this segment needs to be avoided in the process of selecting the optimal spectral regions. The absorption bands corresponding to ethyl octanoate appeared at 5900 cm^{-1}, correlated with the first overtone of the methyl (-CH$_3$) group; while at 5770 and 5670 cm^{-1}, it is associated with the first overtone of the methylene (-CH$_2$) group (Han *et al.*, 2016). Therefore, this spectral region should be taken into consideration for establishing the NIR model of ethyl octanoate. Figure 1(B) illustrates the original spectra pre-processed with SNV, with a selected spectral region from 6101.7 to 5449.8 cm^{-1}, which removed irrelevant information, and improved the operation efficiency and model stability.
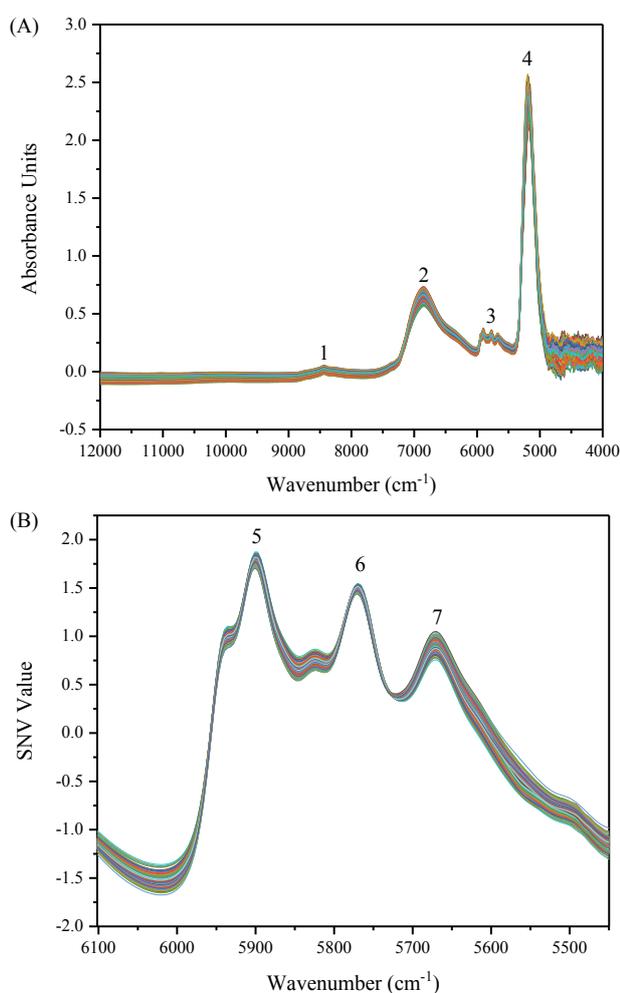

Figure 1. NIR spectra of all liquor samples. (A) Original spectra; (B) Spectra pre-processed with SNV. 1: second overtone stretch of C-H; 2: O-H first overtone; 3: first overtone stretch of C-H; 4: O-H combination band; 5: first overtone of -CH$_3$; 6 and 7: first overtone of -CH$_2$.

Calibration and validation using NIR spectroscopy

Based on spectral variables and chemical values, the NIR mathematical model was established using PLS regression. The optimal pre-processing method and optimal spectral regions were selected based on the "optimisation function" of the OPUS software. Table 2 lists the effects of eight models built with different pre-processing methods and varied spectral regions. It can be seen from the table that most models were set up in the spectral region of 6101.7 - 5449.8 cm^{-1}. This is consistent with the above NIR spectrum analysis results, which showed that 6101.7 - 5449.8 cm^{-1} might be the characteristic spectral region of the ethyl octanoate model, and could achieve good results by directly using the original spectrum variables (none pre-processing) to participate in modelling. The model built after pre-processing by SNV, MSC, and MMN could achieve better evaluation results than the original spectrum model, because these pre-processing methods could eliminate spectral differences between samples caused by scattering. However, the modelling effect after derivative pre-processing (D1 or D2 pre-processing) was not so good as the effect without pre-processing, as it might be attributed to signals that were not amplified, but spectral noises increased after derivative pre-processing. By comparison, the pre-processing method selected in the final modelling was SNV, and the optimal spectral region was 6101.7 - 5449.8 cm^{-1}.

The number of factors that participated in regression should be properly selected for constructing a PLS model. If there are too many or too few PLS factors, the calibration model may not accurately depict the behaviours of the components. The optimal number of PLS factors for each model was determined by internal cross-validation using the calibration model. A total of 20 PLS factors were introduced into the PLS model for factor optimisation. Figure 2 presents how *R²* and RMSECV of the calibration model built with the SNV pre-processing method interact with increasing PLS factors. The most ideal curve is that RMSECV first decreases rapidly with the increase in the number of PLS factors, the minimum value is reached, and then RMSECV increases slightly. Usually, the number of PLS factors with the smallest RMSECV is chosen. The relationship between *R²* and the number of PLS factors was just opposite to the relationship between RMSECV and the number of PLS factors (reverse curve). The ideal situation was to increase it with the increase in the number of PLS factors at first, and then gradually decrease after the maximum value appeared (Moser *et al.*, 2015).

Table 2. Results of NIR models with different pre-processing methods and spectral regions.

Pre-processing method	Spectral region	Number of PLS factor	Calibration set		Validation set	
			R^2	RMSECV	R^2	RMSEP
None	6101.7 - 5449.8	17	0.9397	4.32	0.9475	3.86
SNV	6101.7 - 5449.8	11	0.9507	3.91	0.9537	3.62
MSC	6101.7 - 5449.8	11	0.9496	3.95	0.9525	3.66
MMN	6101.7 - 5449.8	11	0.9492	3.97	0.9520	3.69
SLS	7501.7 - 5449.8	16	0.9124	3.38	0.9421	4.05
D1	6101.7 - 5449.8	16	0.9388	4.35	0.9197	4.77
D2	7501.7 - 5449.8	15	0.8592	6.61	0.9001	5.32
D1+SNV	9403.2 - 7497.9 6101.7 - 5449.8	14	0.8956	5.69	0.9177	4.83

SNV: standard normal variate; MSC: multiplicative scatter correction; MMN: min-max normalisation; SLS: straight line subtraction; D1: first derivative; D2: second derivative.
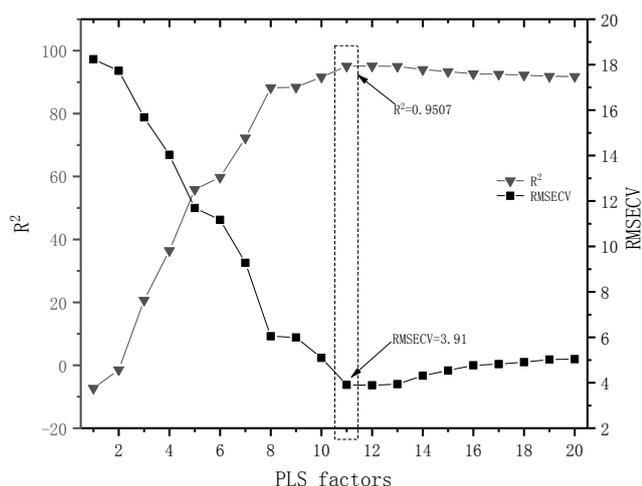

Figure 2. Results of calibration models based on different numbers of PLS factors.

Therefore, it can be seen from Figure 2 that the optimal number of PLS factors should be set as 11 in the calibration model with the SNV pre-processing method.

To illustrate the robustness of the model, the predicted values were plotted against the measured values. Figure 3(A) reveals the correlation between the predicted values and measured values obtained after the calibration set samples were internally cross-validated. It can be observed that the calibration set samples were evenly distributed on both sides of the regression line, indicating that the NIR spectra of ethyl octanoate had a strong linear correlation with its chemical values. R^2 of the model was 0.9507, and RMSECV was 3.91 mg L^{-1}. These results showed that the mathematical statistics of the model reached the most expected value, with R^2
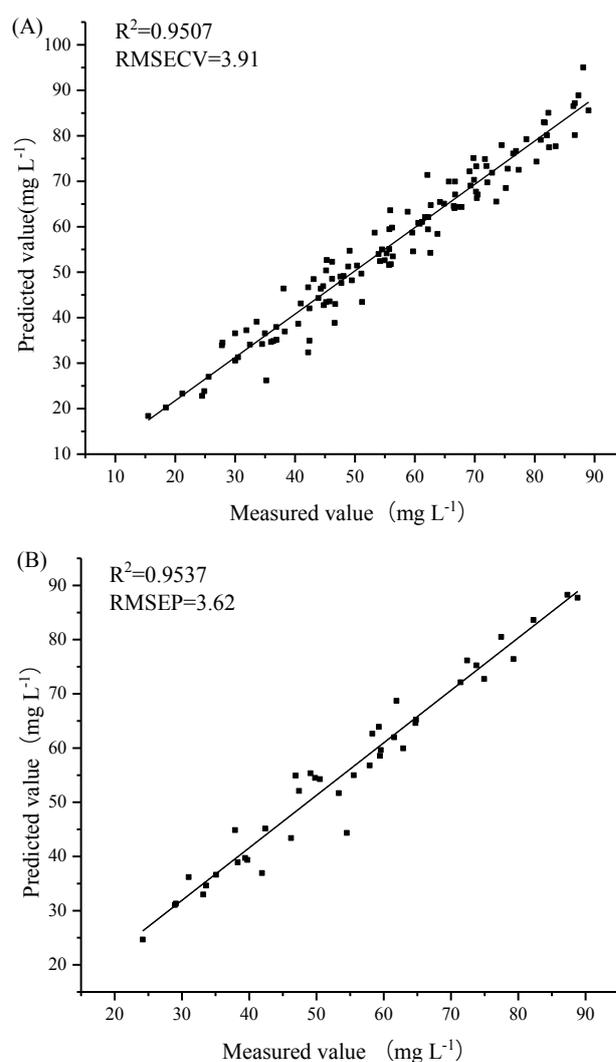

Figure 3. Correlation between predicted values and measured values of ethyl octanoate in the calibration set (A) and validation set (B).

close to 1, and RMSECV being small.

The regression coefficients of the optimal PLS model for ethyl octanoate were plotted in Figure 4. There were strong peaks and troughs for the selected effective wavenumbers (6101.7 - 5449.8 cm^{-1}). As can be seen, the correlation of the chemical values measured by GC-FID with those estimated for ethyl octanoate by the calibration model was excellent. It was found that a high regression coefficient was observed at the wavenumber of 5900 cm^{-1}, which might be linked to the first overtone of -CH$_3$, while the wavenumbers of 5770 and 5670 cm^{-1} could be linked to the first overtone of -CH$_2$. These conclusions are consistent with the analysis results of the original spectra of the liquor samples. The results demonstrated that NIR spectroscopy provided a good prediction model for the ethyl octanoate content in Chinese liquor samples.
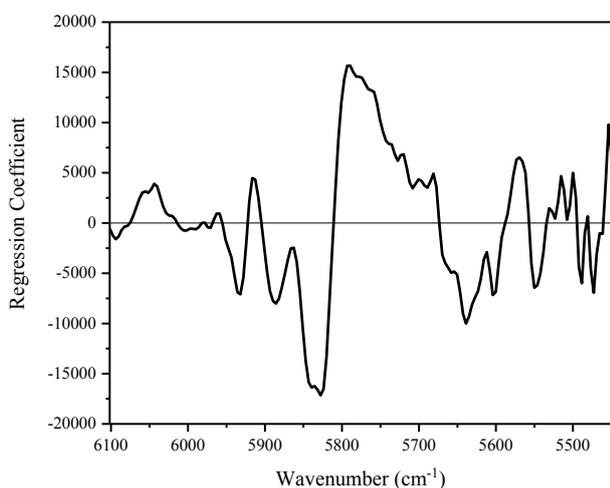

Figure 4. Regression coefficients of the optimal PLS model for ethyl octanoate in Chinese liquor.

After the calibration model was established, external validation by the validation set was required to ensure the applicability of the model. Figure 3(B) shows the correlation of the predicted value with the measured value by external validation. R^2 of the validation set was 0.9537, and RMSEP was 3.62 mg L^{-1}. The correlation and deviation between the NIRS results in of all the samples, and the results of the reference methods met the reproducibility requirements. The predicted value was basically consistent with the chemical value measured by GC-FID, and the prediction effect of the model was satisfactory, which could meet the test requirements in the production of the liquor industry.

Conclusion

In the present work, 162 Chinese liquor

samples were scanned by FT-NIR spectroscopy, and the contents of ethyl octanoate were determined by GC-FID to establish a NIR model for rapid detection of ethyl octanoate in Chinese liquor. The experimental results confirmed the FT-NIR capability to predict the content of ethyl octanoate in Chinese liquor. When compared with traditional GC methods, the NIR technique is a non-destructive and rapid method with no need for previous treatment of samples, and having no contamination issues. It is an ideal rapid detection technology suitable for online quality control of industrial liquor production.

References

Adedipe, O. E., Johanningsmeier, S. D., Truong, V. D. and Yencho, G. C. 2016. Development and validation of a near infrared spectroscopy method for prediction of acrylamide content in French-fried potato. Journal of Agricultural and Food Chemistry 64(8): 1850-1860.

Aleixandre-Tudo, J. L., Nieuwoudt, H., Olivieri, A., Aleixandre, J. L. and du Toit, W. 2018. Phenolic profiling of grapes, fermenting samples and wines using UV-Visible spectroscopy with chemometrics. Food Control 85: 11-22.

Bernhard, T., Truberg, B., Friedt, W., Snowdon, R. and Wittkop, B. 2016. Development of near-infrared reflection spectroscopy calibrations for crude protein and dry matter content in fresh and dried potato tuber samples. Potato Research 59(2): 149-165.

Callado, C. S. C., Nunez-Sanchez, N., Casano, S. and Ferreiro-Vera, C. 2018. The potential of near infrared spectroscopy to estimate the content of cannabinoids in *Cannabis sativa* L.: a comparative study. Talanta 190: 147-157.

Chen, H., Tan, C., Wu, T., Wang, L. and Zhu, W. 2014. Discrimination between authentic and adulterated liquors by near-infrared spectroscopy and ensemble classification. Spectrochimica Acta Part A - Molecular and Biomolecular Spectroscopy 130(17): 245-249.

Chu, Z., Ning, X., Luo, L., Fei, L., Kong, W., Lei, F. and Yong, H. 2014. Detection of aspartic acid in fermented cordyceps powder using near infrared spectroscopy based on variable selection algorithms and multivariate calibration methods. Food and Bioprocess Technology 7(2): 598-604.

Egidio, V. D., Sinelli, N., Giovanelli, G., Moles, A. and Casiraghi, E. 2010. NIR and MIR spectroscopy as rapid methods to monitor red wine fermentation. European Food Research and Technology 230(6): 947-955.

Fan, W., Shen, H. and Xu, Y. 2011. Quantification of volatile compounds in Chinese soy sauce aroma type liquor by stir bar sorptive extraction and gas chromatography-mass spectrometry. Journal of the Science of Food and Agriculture 91(7): 1187-1198.

Fan, W., Yan, X. and Qian, M. C. 2012. Identification of aroma compounds in Chinese "Moutai" and "Langjiu" liquors by normal phase liquid chromatography fractionation followed by gas chromatography/olfactometry. In Qian, M. C. and Shellhammer, T. H. (eds). Flavor Chemistry of Wine and Other Alcoholic Beverages, p. 303-338. United States: American Chemical Society (ACS).

Fei, S., Yang, D., Ying, Y., Zheng, Y. and Tao, J. 2012. Discrimination between Shaoxing wines and other Chinese rice wines by near-infrared spectroscopy and chemometrics. Food and Bioprocess Technology 5(2): 786-795.

Gao, W., Fan, W. and Xu, Y. 2014. Characterization of the key odorants in light aroma type Chinese liquor by gas chromatography-olfactometry, quantitative measurements, aroma recombination, and omission studies. Journal of Agricultural and Food Chemistry 62(25): 5796-5804.

Grassi, S., Amigo, J. M., Lyndgaard, C. B., Foschino, R. and Casiraghi, E. 2014. Beer fermentation: monitoring of process parameters by FT-NIR and multivariate data analysis. Food Chemistry 155(4): 279-286.

Han, S., Zhang, W., Li, X., Li, P., Liu, J., Luo, D. and Xu, B. 2016. Rapid determination of ethyl pentanoate in liquor using Fourier transform near-infrared spectroscopy coupled with chemometrics. Spectroscopy Letters 49(7): 464-468.

Li, Z., Wang, P. P., Huang, C. C., Shang, H., Pan, S. Y. and Li, X. J. 2014. Application of Vis/NIR spectroscopy for Chinese liquor discrimination. Food Analytical Methods 7(6): 1337-1344.

Liu, H. L. and Sun, B. G. 2018. Effect of fermentation processing on the flavor of baijiu. Journal of Agricultural and Food Chemistry 66(22):

5425-5432.

Lorenzo, C., Garde-Cerdán, T., Pedroza, M. A., Alonso, G. L. and Salinas, M. R. 2009. Determination of fermentative volatile compounds in aged red wines by near infrared spectroscopy. Food Research International 42(9): 1281-1286.

Martelovidal, M.J. and Vázquez, M. 2014. Evaluation of ultraviolet, visible, and near infrared spectroscopy for the analysis of wine compounds. Czech Journal of Food Sciences 32(1): 37-47.

Moser, J. K., Singh, M., Rennick, K. A., Bakota, E. L., Jham, G. N., Liu, S. X. and Vaughn, S. F. 2015. Detection of corn adulteration in Brazilian coffee (*Coffea arabica*) by tocopherol profiling and NIR spectroscopy. Journal of Agricultural and Food Chemistry 63(49): article ID 10662.

Niu, Y., Dan, Y., Xiao, Z., Zhu, J., Song, S. and Zhu, G. 2015. Use of stir bar sorptive extraction and thermal desorption for gas chromatography-mass spectrometry characterization of selected volatile compounds in Chinese liquors. Food Analytical Methods 8(7): 1771-1784.

Niu, Y., Yao, Z., Xiao, Q., Xiao, Z., Ma, N. and Zhu, J. 2017. Characterization of the key aroma compounds in different light aroma type Chinese liquors by GC-olfactometry, GC-FPD, quantitative measurements, and aroma recombination. Food Chemistry 233: 204-215.

Ouyang, Q., Zhao, J. and Chen, Q. 2015. Measurement of non-sugar solids content in Chinese rice wine using near infrared spectroscopy combined with an efficient characteristic variables selection algorithm. Spectrochimica Acta Part - A Molecular and Biomolecular Spectroscopy 151: 280-285.

Sha, S., Chen, S., Qian, M., Wang, C. and Xu, Y. 2016. Characterization of the typical potent odorants in Chinese roasted sesame-like flavor type liquor by headspace solid phase microextraction-aroma extract dilution analysis, with special emphasis on sulfur-containing odorants. Journal of Agricultural and Food Chemistry 65(1): 123-131.

Wang, P. P., Li, Z., Qi, T. T., Li, X. J. and Pan, S. Y. 2015. Development of a method for identification and accurate quantitation of aroma compounds in Chinese Daohuaxiang liquors based on SPME using a sol–gel fibre. Food Chemistry 169: 230-240.

Wang, X., Fan, W. and Xu, Y. 2014. Comparison on aroma compounds in Chinese soy sauce and strong aroma type liquors by gas chromatography–olfactometry, chemical quantitative and

odor activity values analysis. European Food Research and Technology 239(5): 813-825.

Wu, Z. Z., Long, J., Xu, E., Wu, C. S., Wang, F., Xu, X. M., ... and Jiao, A. Q. 2015c. Application of FT-NIR spectroscopy and FT-IR spectroscopy to Chinese rice wine for rapid determination of fermentation process parameters. Analytical Methods 7(6): 2726-2737.

Wu, Z., Long, J., Xu, E., Wu, C., Wang, F., Xu, X., ... and Jiao, A. 2015a. Application of FT-NIR spectroscopy and FT-IR spectroscopy to Chinese rice wine for rapid determination of fermentation process parameters. Analytical Methods 7(6): 2726-2737.

Wu, Z., Xu, E., Fang, W., Jie, L., Jiao, X. X. A., Jin, Z., ... and Jie, L. 2015b. Rapid determination of process variables of Chinese rice wine using FT-NIR spectroscopy and efficient wavelengths selection methods. Food Analytical Methods 8(6): 1456-1467.

Ye, M., Yue, T., Yuan, Y. and Zhao, L. 2014. Application of FT-NIR spectroscopy to apple wine for rapid simultaneous determination of soluble solids content, pH, total acidity, and total ester content. Food and Bioprocess Technology 7(10): 3055-3062.

Zheng, Y., Sun, B., Zhao, M., Zheng, F., Huang, M., Sun, J., … and Li, H. 2016. Characterization of the key odorants in Chinese Zhima aroma-type baijiu by gas chromatography-olfactometry, quantitative measurements, aroma recombination, and omission studies. Journal of Agricultural and Food Chemistry 64(26): 5367-5374.

Zhong, J. and Qin, X. 2016. Rapid quantitative analysis of corn starch adulteration in konjac glucomannan by chemometrics-assisted FT-NIR spectroscopy. Food Analytical Methods 9(1): 61-67.